Inorganic Chemistry Communications 13 (2010) 809–813

Contents lists available at ScienceDirect

Inorganic Chemistry Communications

journal homepage: www.elsevier.com/locate/inoche

Coordination-directed one-dimensional coordination polymers generated from a new unsymmetrical oxadiazole bridging ligand and transition metal ions

Zhi-Gang Song, Cui-Hong Geng, Jian-Ping Ma, Yu-Bin Dong *

College of Chemistry, Chemical Engineering and Materials Science, Key Lab of Molecular and Nano Probes Engineering Research Center of Pesticide and Medicine Intermediate Clean Production, Ministry of Education, Shandong Normal University, Jinan, 250014, P.R. China

ARTICLE INFO

Article history:
Received 12 January 2010
Accepted 18 March 2010
Available online 29 March 2010

Keywords:
Unsymmetrical oxadiazole ligand
Crystal structures
One-dimensional chain
Photoluminescence

ABSTRACT

Three one-dimensional coordination polymers, namely $[Zn\mathbf{L}_2(NO_3)_2]_n$ (**1**), $[Cd\mathbf{L}_2(NO_3)_2]_n$ (**2**) and $\{[Zn\mathbf{L}_2(H_2O)_2](ClO_4)_2\bullet 2\mathbf{L}\bullet 2(H_2O)\}_n$ (**3**), have been successfully synthesized based on a new unsymmetrical oxadiazole bridging ligand 2-[2-((3-pyridyl)methoxy)phenyl]-5-[(4-pyridyl)]-1,3,4-oxadiazole (**L**). Compounds **1–3** feature a similar one-dimensional infinite chain that consists of $M_2\mathbf{L}_2$ building block (M = Zn(II) and Cd(II)). In **3**, the uncoordinated **L** ligands are located between the $[M_2\mathbf{L}_2]_n$ chains and serve as the agents to cross-link the chains by weak π–π and H-bonding interactions into a 2D network. In addition, the luminescent properties of **L** and **1–3** were primarily investigated in the solid state.

During the past decades, pronounced interest has been focused on new coordination polymers due to their interesting structures and potential applications in sensing, photoluminescence, ion exchange, separations, gas storage, or catalysis [1,2]. In this context, the design and synthesis of specific organic ligands are foundational issues, because they are some of the most important factors in determining the ultimate structures that are related to their corresponding physical and chemical properties [3].

Recently, our research group has provided a series of bent rigid and flexible organic ligands bridged by five-membered heterocycles for the assembly of polymeric and discrete metal–organic assemblies [4]. As these bent organic spacers possess of variational conformations (cis, trans, or any intermediary conformations between them), this alternative ligand-directed approach has resulted in various coordination metal–organic frameworks with novel patterns not easily achievable by linear ligands. Moreover, heteroatoms such as N and O with free electron pairs on the five-membered heterocyclic rings could be considered as potential active coordination sites and/or hydrogen bond acceptors to expand the polymeric frameworks with additional coordinating and/or hydrogen-bonding interactions to higher dimensionality.

As an in-depth analysis and part of our systemic investigation of self-assembly based on the bent ligands of this type, we herein present three new zinc(II) and cadmium(II) coordination polymers based on a new unsymmetrical ligand **L** [5]. All three new compounds have been fully characterized by IR spectroscopy, elemental analysis, X-ray powder (Fig. 6a) and single-crystal diffractions [6]. In addition, the photoluminescence properties of **1–3** are primarily investigated in the solid state.

Single-crystal structure revealed that **1** contains only one crystallographically independent Zn(II) atom. As shown in Fig. 1, each Zn(II) center adopts a 4 + 2 pseudooctahedral $\{ZnN_4O_2\}$ coordination geometry with the equatorial sites occupied by four N-donors from **L**; the axial positions are occupied by two monodentate coordination nitrate anions. The Zn–N distances range from 2.166(3) Å to 2.197(3) Å, while the axial Zn–O distance is 2.207(3) Å. The Zn–N and Zn–O bond lengths are comparable to those of related compounds [7].

The Zn(II) centers in **1** are connected to each other by **L** to form an infinite 1D chain that consists of a 30-membered bimetallic macrocycle $Zn_2\mathbf{L}_2$ along the *c*-axis. In each rectangle-like ring, the Zn(II) Zn(II) distance is around 13.1 Å (Fig. 2). These 1D chains stack to each other to generate a 2D sheet *via* interchain π–π interactions ($d_{\pi-\pi} = \sim 3.4$ Å) along the direction which is perpendicular to the chains (Fig. 3a). The interchain π–π interactions are resulted from the parallel stacking of the central oxadiazole rings. The shortest interchain Zn(II) Zn(II) distance is ~7.9 Å. Additionally, these π–π interaction-driven 2D sheets are stack in a -ABAB- fashion and linked together through interlayer π–π interaction ($d_{\pi-\pi} = \sim 3.73$ Å), which is resulted from the parallel stacking of one of the terminal pyridyl rings (Fig. 3b), into a 3D network. The shortest interlayer Zn(II) Zn(II) distance is ~9.1 Å (Fig. 3b). Notably, no significant H-bonding interactions have been found in **1**.

2 and **1** are isostructural, and they feature the same 1D infinite chain that consists of $M_2\mathbf{L}_2$ building block. The Cd–N distances range

---

* Corresponding author.
E-mail address: yubindong@sdnu.edu.cn (Y.-B. Dong).

1387-7003/$ – see front matter © 2010 Elsevier B.V. All rights reserved.
doi:10.1016/j.inoche.2010.03.032

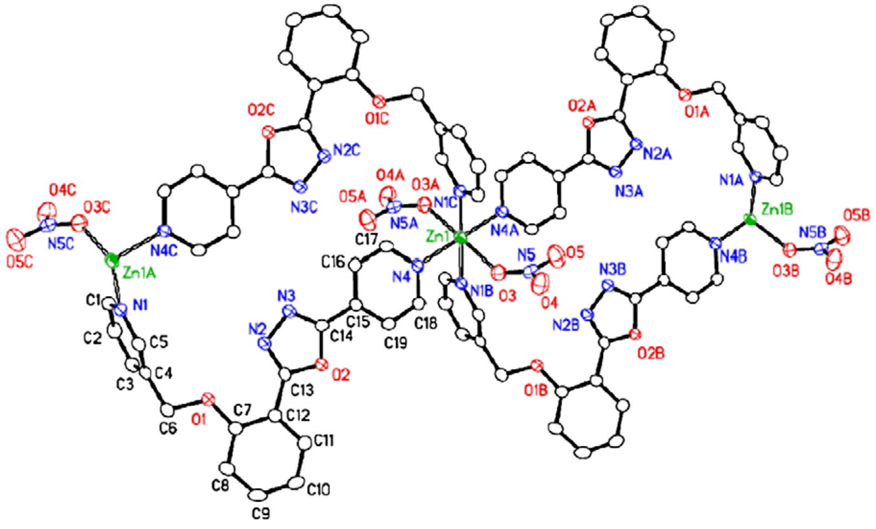

Fig. 1. The coordination environment of Zn(II) atom in **1**, drown with 30% probability ellipsoids. Hydrogen atoms are omitted for clarity.

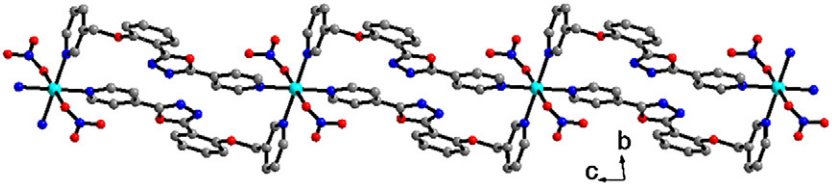

Fig. 2. The 1D double chain of **1** (running along the *c*-axis).

from 2.335(3) to 2.371(3) Å, while the axial Cd–O distances are 2.363 (5) and 2.371(3) Å. The found Cd–N and Cd–O bond lengths in **2** are comparable to those of reported compounds. The corresponding centroid-to-centroid distance between parallel central oxadiazole rings is ca. 3.32 Å, while the centroid-to-centroid distance between the parallel pyridyl rings is ca. 3.74 Å [7] (Fig. 4).

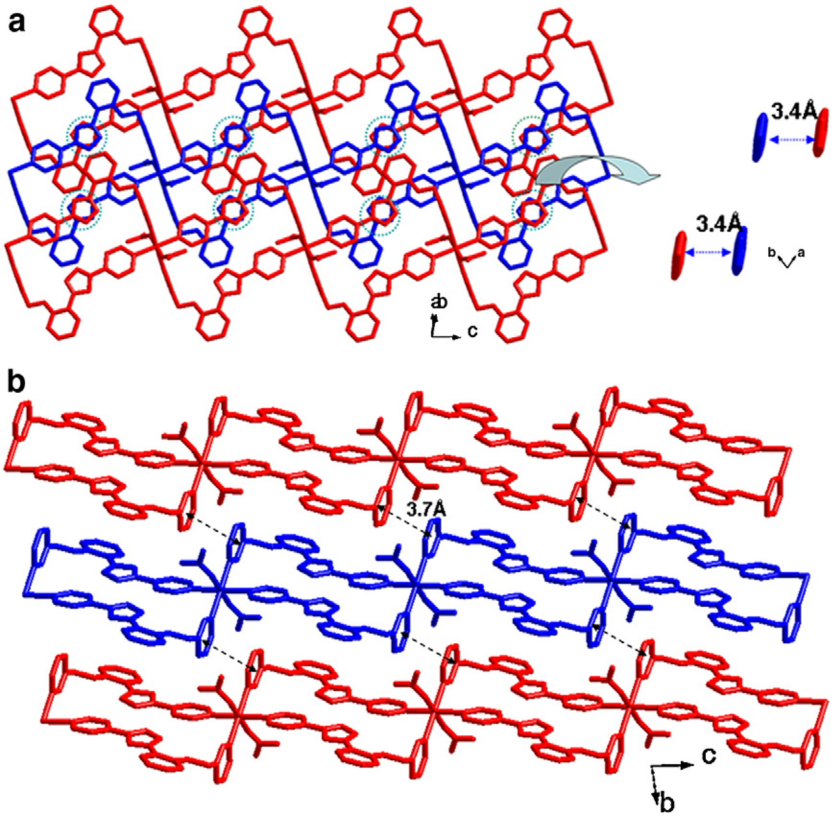

Fig. 3. (a) The 2D sheet driven by interchain π–π interactions. (b) The 3D network driven by the interlayer π–π interactions.

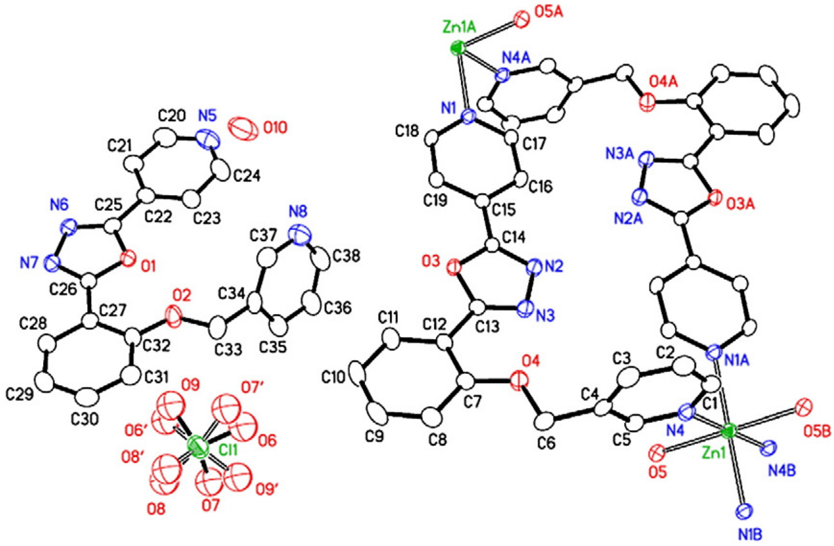

Fig. 4. ORTEP figure of **3** (displacement ellipsoids drawn at 30% probability level).

For studying the impact of various counterions on the self-assembly based on **L**, the weakly coordinated ClO_4^- was used instead of NO_3^-. Crystallization of **L** with $ZnClO_4$ in the same solvent system at room temperature produced compound **3**. Compared to **1**, the Zn(II) center in **3** adopts a similar distorted octahedral $\{ZnN_4O_2\}$ coordination sphere. The axial positions, however, are occupied by two coordinated water molecules instead of coordinated anions found in **1**. The Zn–N distances (ranging from 2.174(3) Å to 2.218(3) Å) are slightly longer that those of **1**, while the Zn–O distance (2.152(3) Å) is slightly shorter than that of **1**. Again, a similar 1D chain composed of the Zn_2**L**$_2$-macroring was found in **3** (Fig. 5a). The uncoordinated ClO_4^- counterions are located between the chains and hydrogen bonded to the uncoordinated water molecules (Fig. 5a).

The most important structural feature in **3** is that there are two (per formula) uncoordinated crystallographically independent **L** spacers. It is worthwhile to point out that, in this specific reaction, the product does not depend on the ligand-to-metal ratio. As shown in Fig. 5a, these 1D chains are linked together by the interchain hydrogen-bonding system which is consisting of the coordinated water molecules, free **L** ligands and uncoordinated water molecules.

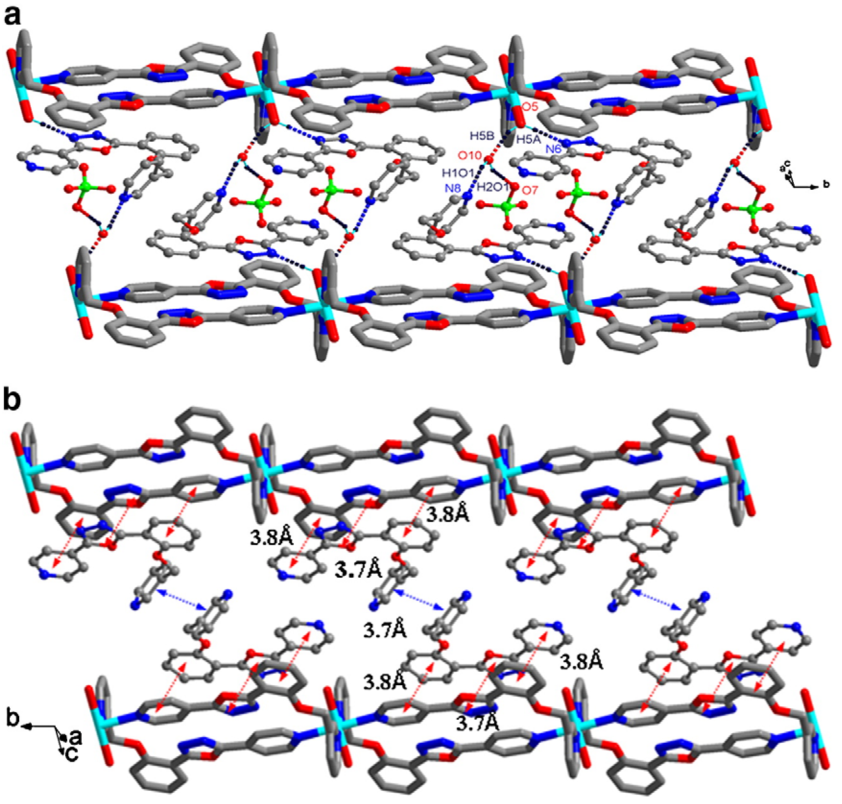

Fig. 5. (a) The hydrogen bonds system between free **L**, H_2O, ClO_4^- and coordinated H_2O in **3**. (b) The π–π interactions between the chains and free **L** in **3**.

Table 1
Geometrical parameters of hydrogen bonds in **3**.

Atom involved	D–H/Å	H···A/Å	D···A/Å	Angle of D–H···A/°
O(10)–H(2O1)...O(9′)v	0.84	2.25	3.039(12)	155.7
O(10)–H(2O1)...O(7)v	0.84	2.04	2.841(10)	158.3
O(10)–H(1O1)...N(8)vi	0.86	2.14	2.945(6)	155.6
O(5)–H(5A)...N(6)vii	0.87	1.98	2.853(4)	177.5
O(5)–H(5B)...O(10)viii	0.79	1.93	2.673(5)	155.3

Symmetry codes: (i) $x,y-1,z$; (ii) $-x+2,-y+2,-z$; (iii) $x,y+1,z$; (iv) $-x+2,-y+1,-z$; (v) $-x+1,-y+1,-z+1$; (vi) $x-1,y,z$; (vii) $-x+2,-y+1,-z+1$; (viii) $x+1,y+1,z$.

The corresponding hydrogen bonds parameters for **3** are listed in Table 1. Furthermore, the interchain π–π interactions ($d_{\pi-\pi}=3.7$–3.8 Å) also exist in **3**, which is composed of the coordinated and uncoordinated **L** ligands. In **3**, the free **L** organic spacers serve as the effective agents that allow weak π–π stacking and hydrogen-bonding interactions to expand the dimensionality of **3** from one to two.

It is noteworthy that compounds **1–3** are obtained as pure phase, which is well confirmed by the X-ray powder diffraction. As shown in Fig. 6, the XRPD patterns of **1–3** obtained from the bulk crystalline solid are identical to those of simulated ones based on the single crystals.

Syntheses of inorganic–organic coordination polymers by the judicious choice of conjugated organic spacers and transition metal centers have been proven to be an efficient method for obtaining new types of luminescent materials [8]. The photoluminescence property of these three new compounds as well as the free ligand was examined in the solid state at room temperature. Upon excitation at $\lambda=348$ nm, **L** exhibits one emission maximum at 409 nm, while **1–3** provide their emission maxima at 457, 429 and 460 nm, respectively (Fig. 7). The red-shift luminescence of **1–3** originates from ligand-to-metal-charge transfer (LMCT). Notably, in the cases of **2** and **3**, almost identical emission bands are observed, thus, the different emission colors of **1–3** might be caused by the different involved metal ions.

We are currently expanding the results presented here by preparing new unsymmetrical ligands of this type with different substituted organic functional groups. We anticipate this approach to be useful for the construction of a variety of new coordination polymers with interesting fluorescent properties.

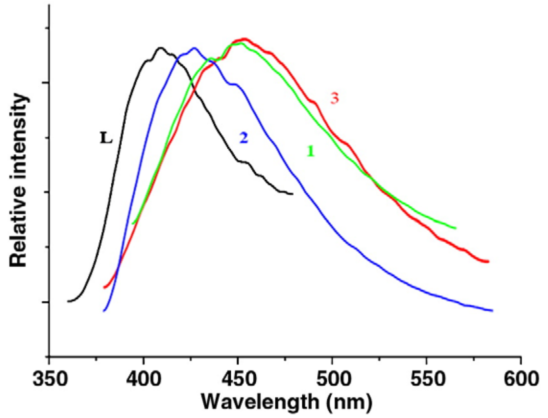

Fig. 7. Solid-state photoinduced emission spectra of **L** and **1–3** at room temperature.

Acknowledgments

We are grateful for financial support from the National Natural Science Foundation of China (grant no. 20871076), the Shandong Natural Science Foundation (grant no. JQ200803), and the Ph.D. Programs Foundation of the Ministry of Education of China (grant no. 200804450001).

Appendix A. Supplementary data

CCDC 760754, 760755 and 760756 contain the supplementary crystallographic data for this paper. These data can be obtained free of charge from The Cambridge Crystallographic Data Centre *via* www.ccdc.cam.ac.uk/data_request/cif.

References

[1] (a) J.R. Long, O.M. Yaghi, Chem. SOC. Rev. 38 (2009) 1203;
(b) P.J. Hagrman, D. Hagrman, J. Zubieta, Angew. Chem., Int. Ed. 38 (1999) 2638;
(c) M. Eddaoudi, D.B. Moler, H. Li, B. Chen, T.M. Reineke, M.O. Keeffe, O.M. Yaghi, Acc. Chem. Res. 34 (2001) 319;
(d) J.S. Seo, D. Whang, H. Lee, S.I. Jun, Y..J. Jeon, K. Kim, Nature 404 (2000) 982.
[2] (a) G.F. Swieger, T.J. Malefetse, Chem. Rev. 100 (2000) 3483;
(b) Y.-B. Dong, M.D. Smith, H.-C. zur Loye, Angew. Chem., Int. Ed. 39 (2000) 4271;
(c) C.-Y. Su, Y.-P. Cai, C.-L. Chen, D.M. Smith, H.-C. zur Loye, J. Am. Chem. Soc. 125 (2003) 8595;
(d) D.L. Caulder, K.N. Raymond, Acc. Chem. Res. 32 (1999) 975;

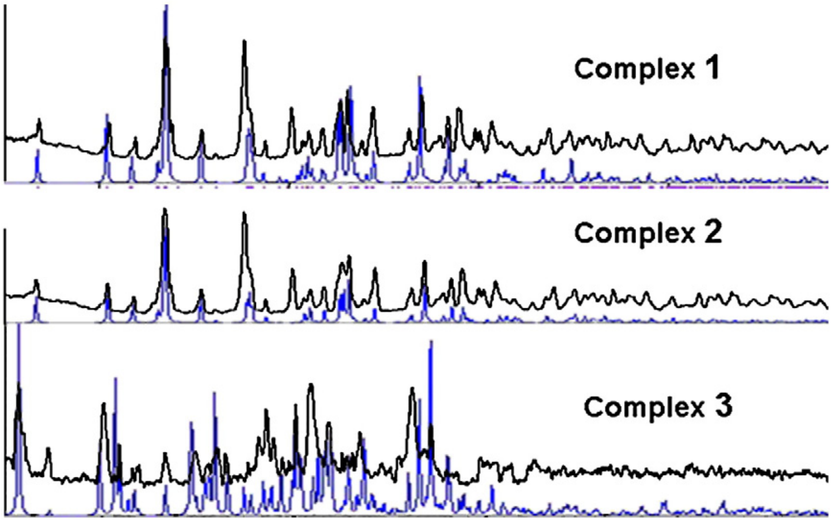

Fig. 6. The XRPD patterns (black lines) obtained from the as-synthesized solids of **1–3** and the simulated XRPD patterns (blue lines) from single crystals of **1–3**.

(e) P. Jacopozzi, E. Dalcanale, Angew. Chem. Int. Ed. Engl. 36 (1997) 613;

(f) J.-F. Wang, E. Ghassan, E. Jabbour, A. Mash, J. Anderson, Y.-D. Zhang, P.A. Lee, R. Neal, N. Armstrong, Peyghambarian, B. Kippelen, Adv.Mater 11 (1999) 1266.

[3] (a) For example, see A.N. Khlobystov, M.T. Brett, A.J. Blake, N.R. Champness, P.M. W. Gill, D.P. O'Neill, S.J. Teat, C. Wilson, M. Schröder, J. Am. Chem. Soc. 125 (2003) 6753;

(b) K. Uemura, S. Kitagawa, M. Kondo, K. Fukui, R. Kitaura, H.-C. Chang, T. Mizutani, Chem. Eur. J. 8 (2002) 3586.

[4] (a) Y.-B. Dong, J.-P. Ma, R.-Q. Huang, M.D. Smith, H.-C. zur Loye, Inorg. Chem. 42 (2003) 294;

(b) Y.-B. Dong, Q. Zhang, L.-L. Liu, J.-P. Ma, B. Tang, R.-Q. Huang, J. Am. Chem. Soc. 129 (2007) 1514;

(c) Y.-B. Dong, P. Wang, J.-P. Ma, X.-X. Zhao, B. Tang, R.-Q. Huang, J. Am. Chem. Soc. 129 (2007) 4872;

(d) P. Wang, J.-P. Ma, Y.-B. Dong, R.-Q. Huang, J. Am. Chem. Soc. 129 (2007) 10620;

(e) G.-G. Hou, J.-P. Ma, T. Sun, Y.-B. Dong, R.-Q. Huang, Chem. Eur. J. 15 (2009) 226;

(f) P. Wang, J.-P. Ma, Y.-B. Dong, Chem. Eur. J. 15 (2009) 10432;

(g) Q.-K. Liu, J.-P. Ma, Y.-B. Dong, Chem. Eur. J. 15 (2009) 10364.

[5] The material 2-(5-(pyridin-4-yl)-1,3,4-oxadiazol-2-yl)phenol was prepared by adopting and modifying the method described in the literature [2 (f)]. ^{1}HNMR (300 MHz, $CDCl_3$, 25 °C, TMS, ppm): 10.06 (s, 1 H), 8.89 (s, 2 H), 8.04 (s, 2 H), 7.88 (d, 1 H), 7.50 (t, 1 H), 7.18 (d, 1 H), 7.09 (t, 1 H); IR (KBr pellet, cm^{-1}): 3040 (w), 1625 (vs), 1591 (s), 1536 (vs), 1487 (vs), 1412 (vs), 1241 (s), 1061 (m), 969 (w), 823 (s), 774 (m), 751 (vs), 705 (vs), 640 (s), 540 (m), 464 (w). Anal. calcd. for $C_{13}H_9N_3O_2$: C 65.27; H 3.79; N 17.56. Found: C 65.24; H 3.82; N 17.52. The ligand **L** was synthesized as follows: 2-(5-(pyridin-4-yl)-1,3,4-oxadiazol-2-yl)phenol (2 mmol, 0.480 g), K_2CO_3 (10 mmol, 1.38 g) and KI (5 mmol, 0.830 g) were added into 20 mL dry DMF with stirring at ambient temperature; then 3-picolyl chloride hydrochloride (2 mmol, 0.255 g) was added to the suspended liquid. The mixture was stirred for 18 h at room temperature (monitored by thin-layer chromatography (TLC)), then added lot of water. The precipitation was separated by filtration, washed several times with water, the residue was purified on a silica gel column using THF as the eluent to afford **L** as a white crystalline solid. Yield: 66%. m.p. 166–168 °C. ^{1}HNMR (300 MHz, $CDCl_3$, 25 °C, MS, ppm): 8.80–8.79 (d, 3 H), 8.60–8.59 (d, 1 H), 8.10–8.08 (d, 1 H), 8.04–8.01 (d, 1 H), 7.81–7.79 (d, 2 H) 7.46–7.23 (t, 1 H), 7.23–7.21 (t, 2 H), 6.85–6.63 (t, 1 H), 5.36 (s, 2 H); IR (KBr pellet, cm^{-1}): 3422 (m) 1602 (s) 1529 (s) 1474 (s) 1414 (s) 1268 (s) 1133 (m) 1000 (m) 831 (m) 788 (s) 745 (s) 708 (s). Anal. calcd. for $C_{19}H_{14}N_4O_2$: C 69.08; H 4.27; N 16.96. Found: C 69.05; H 4.29; N 16.71.

[6] Preparation of **1** and **2**: A methanol solution of **L** (0.010 g, 0.30 mmol) and Zn $(NO_3)_2$ (0.0057 g, 0.30 mmol) or $Cd(NO_3)_2$ (0.0108 g, 0.30 mmol) was left for 5 days at room temperature, **1** (Yield, 73%) and **2** (Yield, 82%) were obtained as colorless crystals. IR data (KBr pellet, cm^{-1}) **1**: 3453 (br, s), 1623 (m), 1537 (m), 1494 (s), 1384 (s), 1167 (s), 1129 (m), 1081 (m), 806 (s), 748 (w), 706 (m), 655 (w). Anal. calcd. for $C_{38}H_{28}N_{10}O_{10}Zn$ (**1**): C 53.68, H 3.32, N 16.48. Found: C 53.70, H 3.29, N 16.51. **2**: 3447 (br, s), 1605 (s), 1532 (m), 1493 (m), 1383 (br, s), 1304 (s), 1257 (m), 1056 (w), 1007 (m), 872 (w), 805 (m), 741 (m). Anal. calcd. for $C_{38}H_{28}N_{10}O_{10}Cd$ (**2**): C 50.88, H 3.15, N 15.61. Found: C 50.90, H 3.12, N 15.63. Preparation of **3**: A methanol solution of **L** (0.010 g, 0.30 mmol) and $Zn(ClO_4)_2$ (0.0079 g, 0.30 mmol) was left for about 3 days at room temperature, **3** (Yield, 87%) was obtained as colorless crystals. IR data (KBr pellet, cm^{-1}) **3**: 3443 (br, s), 1653 (m), 1624 (m), 1538 (m), 1496 (m), 1463 (m), 1432 (m), 1384 (w), 1121 (s), 1108 (vs), 834 (w), 746 (m), 708 (m), 625 (s). Anal. calcd. for $C_{76}H_{64}Cl_2N_{16}O_{20}Zn$ (**3**): C 55.06, H 3.89, N 13.52. Found: C 55.05, H 3.87, N 13.54. X-ray intensity data were measured at 298(2) K on a Bruker SMART APEX CCD-based diffractometer (Mo Kα radiation, $\lambda = 0.71073$ Å). Crystal data for **1**: $C_{38}H_{28}N_{10}O_{10}Zn$, $M = 850.07$, triclinic, space group $P\,1$, $a = 7.940(2)$, $b = 8.955(2)$, $c = 13.097(3)$ Å, $\alpha = 82.819(4)°$, $\beta = 87.585(4)°$, $\gamma = 72.604(3)°$, $V = 881.7(4)$ Å^3, $Z = 1$, final R indices [I>2sigma(I)]: $R1 = 0.0530$, $wR2 = 0.1315$. Crystal data for **2**: $C_{38}H_{28}N_{10}O_{10}Cd$, $M = 897.1$, triclinic, space group $P\,1$, $a = 8.0099(19)$, $b = 8.953(2)$, $c = 13.271(3)$ Å, $\alpha = 82.990(3)°$, $\beta = 87.260(3)°$, $\gamma = 72.370(3)°$, $V = 900.2(4)$ Å^3, $Z = 1$, final R indices [I>2sigma(I)]: $R1 = 0.0425$, $wR2 = 0.0972$. Crystal data for **3**: $C_{76}H_{64}Cl_2N_{16}O_{20}Zn$, $M = 1657.70$, triclinic, space group $P\,1$, $a = 8.9536(17)$, $b = 13.309(3)$, $c = 16.703(3)$ Å, $\alpha = 111.848(3)°$, $\beta = 90.811(3)°$, $\gamma = 95.663(3)°$, $V = 1835.6(6)$ Å^3, $Z = 1$, final R indices [I>2sigma(I)]: $R1 = 0.0701$, $wR2 = 0.1852$.

[7] (a) Y.-B. Dong, J.-P. Ma, M.D. Smith, R.-Q. Huang, B. Tang, D. Chen, H.-C. zur Loye, Solid State Sci. 4 (2002) 1313;

(b) S. Muthu, J.H.K. Yip, J.J. Vittal, J. Chem. Soc. Dalton Trans. (2001) 3577;

(c) L.-N. Zhu, L. Yi, W. Dong, W.-Z. Wang, Z.-Q. Liu, Q.-M. Wang, D.-Z. Liao, Z.-H. Jiang, S.-P. Yan, J. Cood. Chem. 59 (2006) 457;

(d) Z.-Q. Xu, L.K. Thompson, D.A. Black, C. Ralph, D.O. Miller, M.A. Leech, J.A.K. Howard, J. Chem. Soc. Dalton Trans. (2001) 2042;

(e) H.D. Selby, P. Orto, Z.-P. Zheng, Polyhedron 22 (2003) 2999.

[8] (a) D.M. Ciurtin, N.G. Pschirer, M.D. Smith, U.H.F. Bunz, H.-C. zur Loye, Chem, Mater. Des. 13 (2001) 2743;

(b) Y.-B. Dong, J.-P. Ma, R.-Q. Huang, F.-Z. Liang, M.D. Smith, Dalton Trans. 9 (2003) 1472.